Optimal Power Flow in Uncertain Power System

Namami Krishna Sharma, S. C. Choube

Abstract*: Due to the increasing demand of electricity in ever-growing electricity market, it is necessary to observe the nature of load and map the effects of load uncertainties on the operation of power system. These uncertainties have also led to voltage instability which is sooner or later considered to be a fundamental cause of blackouts. The distributed generation sources can also be regarded as the source of uncertainties at the load ends of power systems. Along with the load uncertainties, wind turbine generation (WTG) and solar plants have also been used as a source of uncertainties in this paper. The load uncertainties have been incorporated in the system by designing a dynamic load flow program. Corresponding to all uncertain inputs critical case has been identified by the singularity property of load flow jacobian. For the optimal load flow a multi-objective optimization problem aiming to constrained objective function to enhance voltage stability, improve stability index value, reduce system losses and increase reactive reserve margins at generator buses has been formulated. Black hole algorithm has been used to achieve the optimal values of control variables and hence optimal load flow. The aforementioned problem has been tested on standard IEEE-14 bus system.

Keywords: Load uncertainty, distributed generation, Reactive compensation, optimal power flow, BHA.

NOMENCLATURE

A. ***Parameters***

N	Normal Distribution
exp	Exponential Distribution
db	Base Case load deviation
Ψ	Uncertain load parameter
ξ	Uncertainty results on the output parameters
μ	Average Value
σ	Standard Deviation
λ	linearly distributed parameter

B. ***Constants***

P_{Di}^{0}	Active power load in MW at ith bus at Base case
Q_{Di}^{0}	Reactive power load in Mvar at ith bus at Base case
G_k	Real part of shunt admittanve of line ‘k’ in pu
Y_{ij}	Shunt admittance of the line
θ_{ij}	Angle in degree of Y_{ij}
A	wind turbine’s cross-sectional area in m^2
Φ	WTG Power Factor angle
ρ_a	density of air in kg/m3 (1.225)
C_P	Turbine coefficient (0.5926)
$v_{cut\ \ in}$	Cut-in speed of wind (3.5m/s)
$v_{cut\ \ out}$	Cut-out speed of wind (20m/s)
v_r	Rated wind speed (11m/s)

C. ***Variables***

$P_{Di}(\psi)$	Uncertain Real loading at ith bus
$Q_{Di}(\psi)$	Uncertain Reactive loading at ith bus
V_k^{ξ}	Voltage magnitude in pu due to ψ uncertainties
V_k^{0}	Base case Voltage magnitude
δ_i^{ξ}	Voltage angle due to ψ uncertainties
P_{Gi}^{0}	Base case real power generation at ith generator bus
Q_{Gi}^{0}	Base case reactive power generation at ith bus
P_{Gi}^{ξ}	Real power generation at ith bus due uncertain loads
Q_{Gi}^{ξ}	Reactive power generation ith bus due to uncertain loads
V_i^{ξ}	Voltage magnitude at ith bus in pu due to uncertain load
$P_{WTGi}^{'}$	Real Power supplied by WTG in MW
$Q_{WTGi}^{'}$	Reactive Power drawn by WTG in Mvar
Q_{WTGi}	Resultant Reactive Power load in Mvar at ith PQ bus which is selected for placement of WTG
v	Wind velocity in meter/sec
ΔQ_{Gi}^{res}	Technical reactive reserves in Mvar

I. INTRODUCTION

The nondeterministic or uncertain behavior of loads in modern power systems need to be tackled carefully [1]. Under the presence of numerous uncertainties in the power systems the optimal power flow functionality is affected. At present, power system operators and planners are facing problems to maintain voltage stability due to uncertain increasing demand of electricity by the consumers. [2]. The sources of uncertainty in modern power systems includes, ambiguity in generation, transmission, distribution network, distributed generation, loads, energy reserve or economic factors. Alternators, power transmission lines and power transformer’s models have been ascertained in [3,4]. The model of uncertain load in randomness and time-varying distributed property, could be defined by single or many groups of mathematical equations. Precise load modelling has thus become one of the most worrying issue in power system research field [5, 6]. Under the uncertain environment for the proper and smooth functioning of system operation the available control actions must be utilized effectively and up to its maximum limit to ensure the stability and reliability of the system.

Revised Manuscript Received on January 06, 2020.
*****Correspondence Author
Namami Krishna Sharma, department of Electrical & Electronics Engineering, UIT-RGPV, Bhopal, India, Email: er.namami@gmail.com
S. C. Choube, department of Electrical & Electronics Engineering, UIT-RGPV, Bhopal, India, Email: scchoube@yahoo.com

Sources of uncertainty include fuel price, generation convenience, market forces, capacity of transmission systems, nonlinear load demands, unplanned shedding, weather and other interruptions, etc. these uncertainties can be incorporated in the system by designing a proper probabilistic problem and the shortcomings of deterministic approach can also be overawed [7]. Since the deterministic approach does not account the randomness of the parameters, in such cases for the better handling of these randomness the researchers shifted their approaches from deterministic to probabilistic one. Uncertainties affect the operation of the power system in terms of power transfer capability and voltage stability limits and other operating parameters of the system. The inclusion of load uncertainties by designing a computational feasible method is shown in [9]. Due to the increasing demand of electricity and consequently the penetration of distributed generation [6-9], it has now also become imperative that these renewable energy resources are modelled along with loads. Solar photovoltaic (PV) installations is growing rapidly and affecting load profiles as it replaces a part of the load and/or is as added to production units of distribution system. PV penetration affect the voltage profile, stability, and operation of system [20,21]. In this paper a dynamic load flow model is has been developed to account the randomness of load uncertainties over a certain period of time [8]. Various modern optimization techniques have been used for solving the complex problem given in [10,11]. Black Hole optimization (BHA) technique proposed in [11] is the modified swarm optimization technique is being widely used for solving engineering optimization problem. A voltage stability enhancement analysis under the presence of load uncertainties and distributed generation has been carried out in this paper. A multi-objective optimization problem has been designed aiming to minimize the voltage deviation, L-Index and line losses has been designed in this paper and reactive shunt compensation has been used as control variable. The effectiveness of the proposed technique has been observed by calculating the voltage benefit factors, loss benefit factors and improvement in total reactive reserve in the system [16]. Deviation from base loading at different buses, normally distributed and exponentially distributed load models have been used in this paper [16]. Wind Turbine Generator (WTG) and Solar photovoltaic system have also been modelled in this paper to account the effect of uncertainties due to distributed generation. The stability index (minimum eigen value of load flow Jacobian matrix) has been used as an indicator to identify the critical or adverse case under the given sets of uncertain conditions. After identifying critical case black hole optimization technique has been employed to find optimum value of control variable (VAR compensation) which satisfies the objective functions and all the operating limits. The proposed technique has been implemented on IEEE-14 bus system.

In this paper the overview of Black hole optimization is given in section II. Uncertain load, WTD and solar modelling have been done in section III. Section IV covers the methodology and problem formulation of the proposed problem. Results have been shown in section V and the conclusions are given in the last section.

II. BLACK HOLE OPTIMIZATION

A. Overview

A. Hatamlou [11] has proposed the modified population-based optimization technique inspired from the 'Black Hole' phenomenon. In the journey of a star towards the blackhole, there may be a probability of crossing the event horizon. The stars or candidate solutions which crosses the event horizon they are sucked by the black hole. The black hole optimization problem is formulated as follows:

$$r_i(k+1) = r_i(k) + rand(r_{BH} - r_i(k)) \quad (1)$$

Where $r_i(k+1)$ and $r_i(k)$ are the locations of the star at iterations 't' and 't+1', respectively and r_{BH} is the location of the black hole in the search space, '$rand$' is a random number in the interval [0-1]. N is the number of stars (candidate solutions). Every time a candidate (star) dies, it is sucked in by the black hole, another candidate solution (star) is born and distributed randomly in the search space and starts a new search. In the BHA algorithm the event horizon radius is calculated by following equation:

$$r = \frac{F_{BH}}{\sum_{i=1}^{N} F_i} \quad (2)$$

Where 'f_{BH}' is the fitness value of the black hole and 'fi' is the fitness value of the 'i^{th}' star. When the distance between a candidate solution and the black hole (best candidate) is less than R, that candidate is collapsed and a new candidate is created and distributed randomly in the search space.

III. UNCERTAIN LOAD, WTG AND SOLAR MODELLING

A. Normally distributed uncertain load

Various load models are given in [12,13,14,15]. The normally distributed load modelling is done as follows:

$$P_{D9}(\Psi_N) = Normrnd(\mu_1, \sigma_1, m, n) \quad (3)$$

$$Q_{D9}(\Psi_N) = Normrnd(\mu_2, \sigma_2, m, n) \quad (4)$$

Bus no. 9 is selected for this modelling (with μ_1=30 and σ_1=10, μ_2 =17 and σ_2 =5) and m, n is a (48x1) array. The real and reactive load variations are shown in figures 1 to 4.

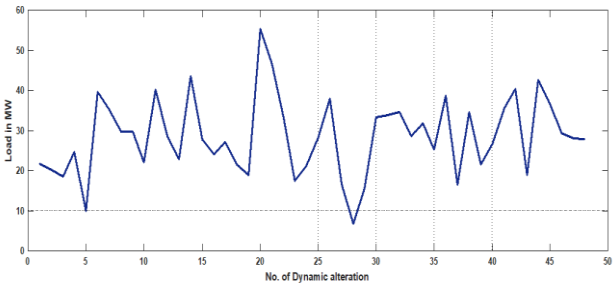

Fig. 1: Variation of real load at bus no. 9

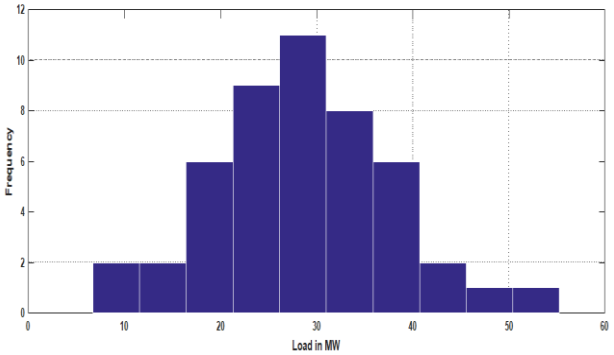

Fig. 2: Histogram of real load Variation at bus no. 9

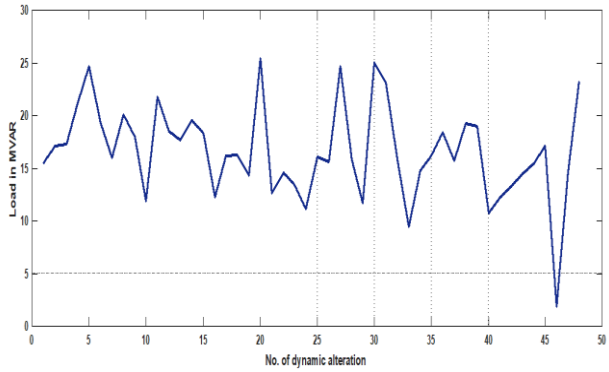

Fig.3: Variation of reactive load at bus no. 9

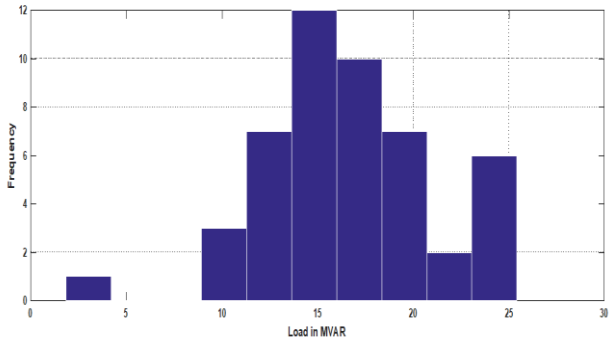

Fig. 4: Histogram of reactive load variation at bus no. 9

B. Exponentially distributed uncertain load

The exponentially distributed uncertain load can be modelled as follows [16]:

$$f(P_{D5}) = \frac{e^{-\frac{(P_{D5}-\mu)}{b}}}{b}$$
$$P_{D5} \geq \mu \quad (5)$$
$$b > 0$$

$$P_{D5}(\Psi_{\exp}) = P_{D5}^{0} + \frac{\exp\frac{(x-\mu)}{b}}{b} \quad (6)$$

with x = linearly spaced numbers between $(0 - P_{D5}^{0})$

b = 1.8

Similarly, for Q_{D5}

$$Q_{D5}(\Psi_{\exp}) = Q_{D5}^{0} + \frac{\exp\frac{(x-\mu)}{b}}{b} \quad (7)$$

Exponentially distributed loads are shown in figures 5 to 8:

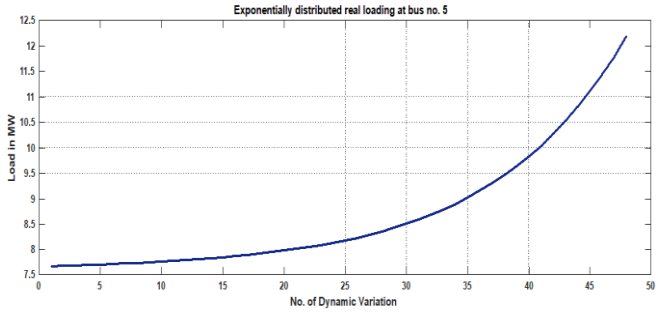

Fig. 5: Variation of real load at bus no. 5

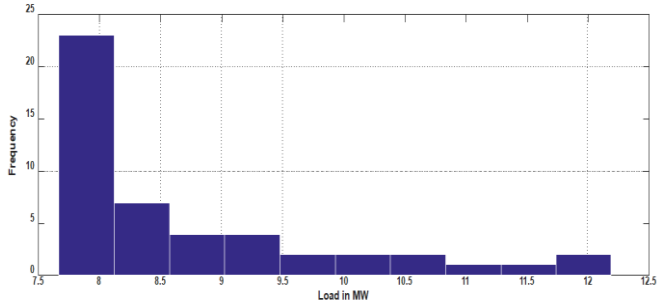

Fig. 6: Histogram of real load variation at bus no. 5

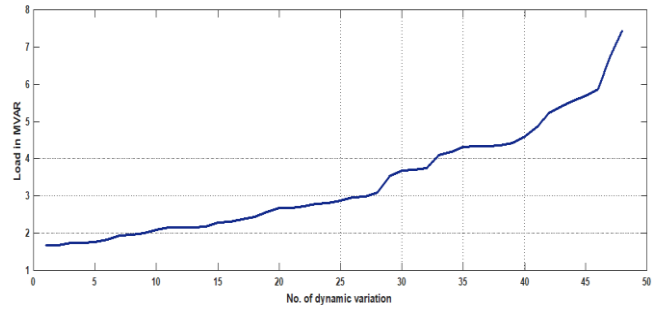

Fig. 7: Variation of reactive load at bus no. 5

C. Deviation from base case loading

Load at bus no. 10 is varying from rated to 150% of rated load values and the modelling is done as follows:

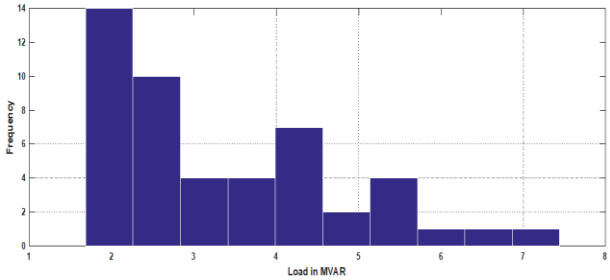

Fig. 8: Histogram of reactive load variation at bus no. 5

(i) Real power loading

$$P_{D10}(\Psi_{db}) = P_{D10}^{0}(1+\lambda) \quad (8)$$

(ii) Reactive load modelling

$$Q_{D10}(\Psi_{db}) = Q_{D10}^{0}(1+\lambda) \quad (9)$$

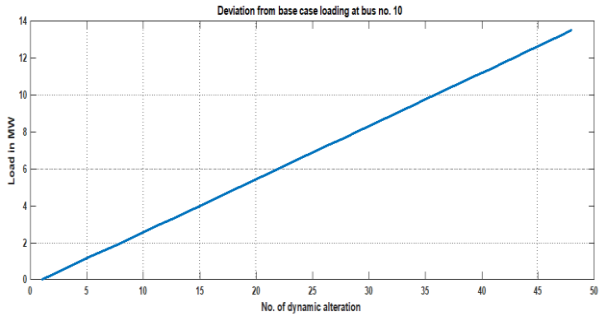

Fig. 9-Variation of real power load at bus no. 10

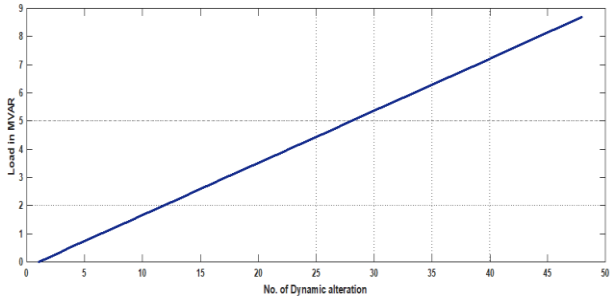

Fig.10-Variation of reactive load at bus no.10

D. Modelling of wind turbine generator

The power generated by (WTG) is a direct function of air velocity and it consumes the reactive power from the grid at the same time [17]. WTG modelling are presented in [18-19]. The operating power factor of WTG is assumed to be constant at (0.95 lag). Placement of WTG units depends on the air flow and other physical parameters. Here bus no. 4 and 7 are chosen as candidate buses for the placement of WTG units.

$$P_{WTGi} = P_{Di}^{0} - P_{DGi}^{'} \;;\; P_{WTGi}^{'} \le 9MW \tag{10}$$

$$Q_{WTGi} = Q_{Di}^{0} + P_{WTGi}^{'} Tan\phi \tag{11}$$

(Cos Φ = 0.9 lagging)

$$P_{WTGi}^{'} = \begin{cases} \frac{1}{2}\rho_a A v^3 C_p \;; & v_{cutin} \le v_{rated} \\ 7.136MW \;; & v_{rated} \le v \le v_{cutout} \end{cases} \tag{12}$$

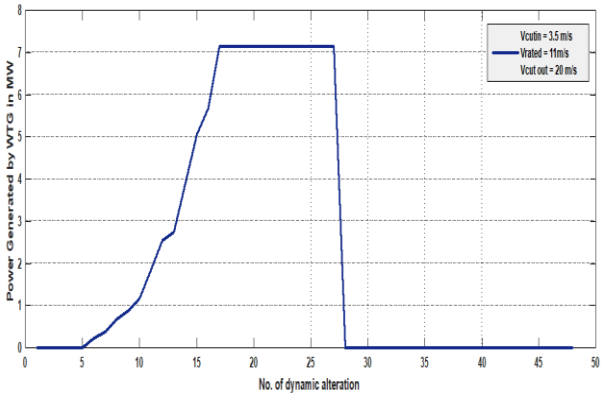

Fig.11: Real power supplied by WTG at bus 4 &7

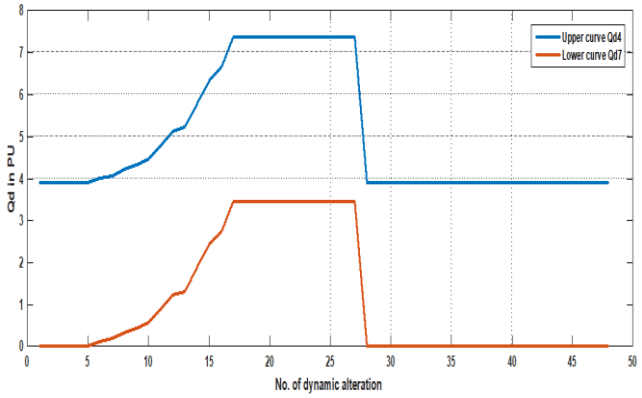

Fig. 12 Reactive power drawn from WTG for buses 4 & 7

E. Modelling of solar photovoltaic system

Solar photovoltaic (PV) installations are growing rapidly and affecting load profiles as it replaces a part of the load and/or is as added to production units of distribution system. PV penetration affect the voltage profile, stability, and operation of system. The electricity generated by a solar photovoltaic system can be estimated as follows:

$$E = A \times r \times H \times PR \tag{13}$$

Where:

E= Energy in KWh

r= solar panel yield (electrical power of one solar panel divided by area of one solar panel in %)

A= Total solar panel area

H= annual average solar radiation

PR= performance ratio (default value 0.75)

Solar output power is given by eq. (14) [20-21] and irradiance variation is taken from [21]. Active power generation at bus 14 where solar generator has been installed is shown in figure 13. Solar array area = 158 m^2 and r=14%.

$$P_{PVi} = \frac{A \times r \times H \times 10^{-6}}{24} \quad \text{MW} \tag{14}$$

IV. METHODOLOGY

Following methodology has been adopted:

(1) Load models for selected load buses have been developed and are incorporated in a dynamic load flow program.

(2) WTG and solar photovoltaic modelling have been done for including the effect of distributed generation.

(3) Run the load flow program for all the dynamic input values and observe the minimum eigen value of load flow Jacobian (exclude those results on which load flow did not converge).

(4) After identifying the critical case an optimization problem based on 'Black Hole Algorithm' has been designed for maintaining system voltage stability and improving the performance of the system.

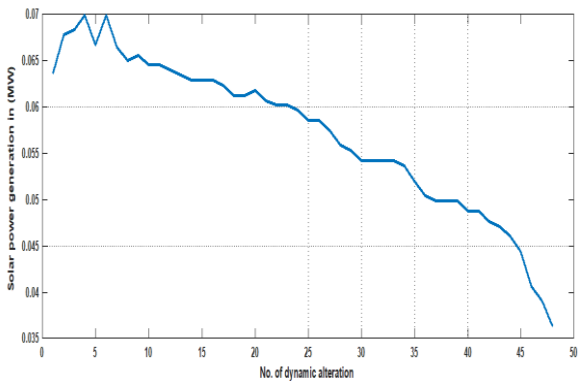

Fig. 13: Solar power output

(5) candidate buses for the placement of reactive shunt compensating units (SVCs) have been found out by L-index (bus) values [22]. L-index varies between 0 to 1. If the index value of any bus approaches to unity means that bus is operating near its stability limit. The buses having the higher values of indexes are chosen as candidate buses. L-index If the L-index approaches to unity means system is approaching towards voltage instability and consequently voltage collapse state.

$$Lindex_k = \max_{k\in\beta_L}\left|1-\frac{\sum_{i\in\beta_G} F_{ki}V_i}{V_k}\right| \quad (15)$$

Where:
$\boldsymbol{\beta}_L$ is the set of load buses and $\boldsymbol{\beta}_G$ is the set of generator buses and F_{ki} is the subset of hybrid matrix, which has been generated by Y-matrix. Stability condition lies between
0 < L-index < l

V. PROBLEM FORMULATION

Objective Functions

Minimum voltage deviation

$$F_1 = \min(abs(1-V_k^{\xi})) \quad (16)$$

Minimum real power loss

$$F_2 = \min\sum_{\forall k}^{N_t} G_k\left[\left(V_i^{\xi}\right)^2 - \left(V_j^{\xi}\right)^2 - 2V_i^{\xi}V_j^{\xi}Cos\left(\delta_i^{\xi} - \delta_j^{\xi}\right)\right] \quad (17)$$

Minimum L index(bus)

$$F_3 = \min(Lindex_j) \quad (18)$$

Subjected to

Equality constraints

$$P_{Gi}^{\xi} - P_{Di}^{\Psi} + P_{DGi}^{'} = \sum_{\forall i}\left|V_i^{\xi}\right|\left|V_j^{\xi}\right|\left|Y_{ij}\right|Cos\left(\theta_{ij} + \delta_i^{\xi} - \delta_j^{\xi}\right) \quad (19)$$

$$Q_{Gi}^{\xi} - Q_{Di}^{\Psi} - Q_{DGi}^{'} = -\sum_{\forall i}\left|V_i^{\xi}\right|\left|V_j^{\xi}\right|\left|Y_{ij}\right|Sin\left(\theta_{ij} + \delta_i^{\xi} - \delta_j^{\xi}\right) \quad (20)$$

Inequality Constraints

$$V_{i\ \min} \le V_i^{\xi} \le V_{i\ \max} \quad (21)$$

(0.95 < V_i <1.05)

$$Q_{Gi\ \min} \le Q_{Gi}^{\xi} \le Q_{Gi\ \max} \quad (22)$$

The uncertainties can be limited by following:

$$\Psi_{\min} \le \Psi \le \Psi_{\max} \quad (23)$$

$$Q_{Gsh\ i\ \min} \le Q_{Gsh\ i} \le Q_{Gsh\ i\ \max} \quad (24)$$

($Q_{Gsh\ i\ min}$ = 0 and $Q_{Gsh\ i\ max}$ = 20 MVAR)

$$\min eig[J] > 0 \quad (25)$$

$$\Delta Q_{gi}^{res} = Q_{Gi\max} - Q_{Gi}^{\xi} \quad (26)$$

Voltage benefit factor and loss benefit factors [16] have also been calculated for checking the effectiveness of the control action:

$$VBF_i = \frac{V_i(Q_{Shi}) - V_{io}}{Q_{shi}} \times 100\% \quad (27)$$

$$LBF_i = \frac{P_{Lo} - P_L(Q_{Shi})}{Q_{shi}} \times 100\% \quad (28)$$

VI. RESULTS AND DISCUSSIONS

Base case load flow results and L-Index for buses of IEEE-14 bus system are shown in Table-I.

Table-I: Base case load flow results of IEEE-14 bus system

Minimum eigen value 0.5976

Bus no.	IVI (pu)	δ (degree)	P_G (MW)	Q_G (MVAR)	L-index
1	1.010	2.153	114.170	10.092	-
2	1.000	0.000	102.289	37.590	-
3	0.980	-5.478	50.000	34.642	-
4	0.957	-5.216	0.000	0.000	0.0343
5	0.961	-4.155	0.000	0.000	0.0233
6	1.000	-10.422	0.000	19.355	-
7	0.976	-8.737	0.000	0.000	0.0443
8	1.000	-8.737	0.000	13.637	-
9	0.961	-10.622	0.000	0.000	0.0785
10	0.960	-10.913	0.000	0.000	0.0748
11	0.976	-10.802	0.000	0.000	0.0422
12	0.982	-11.396	0.000	0.000	0.0279
13	0.975	-11.436	0.000	0.000	0.0376
14	0.947	-12.165	0.000	0.000	**0.0911**
Total P_G =266.459 MW			**Total Q_G** = 115.316 MVAR		
Total P_D = 259.300 MW			**Total Q_D** = 81.400 MVAR		
Total P_{loss} = 7.163 MW			**Total Q_{loss}** = 33.918 MVAR		

L-index was presented by Kessel and Glavitsch [22], and developed by Jasmon and Lee [23]. The L-index of any branch connected between buses i and j can be expressed by eq. (29)

$$L_{ij} = \frac{4\left[\left(P_jX_{ij} - Q_jR_{ij}\right)^2 + \left(P_jR_{ij} + Q_jX_{ij}\right)V_i^2\right]}{V_i^4} \quad (29)$$

L-index values have been calculated by eq. (29) and are given in table II. These values are calculated for base case to obtain the optimum locations for the placement of WTG. Buses 4 & 7 which connect the line 8 are chosen as candidate buses for the placement of WTGs because L-index value of line 8 is highest amongst all the line values.

Table-II: L-index for lines corresponding to base case

Line no.	L-index	Line no.	L-index	Line no.	L-index
1	0.0309	8	**0.1209**	15	0.0542
2	0.1183	9	0.0563	16	0.0048
3	0.0255	10	0.0481	17	0.0512
4	0.1175	11	0.0939	18	0.0681
5	0.0123	12	0.0685	19	0.0283
6	0.0906	13	0.0952	20	0.1093
7	0.0173	14	0.1009	L-Index (lines)	

Table-III load flow results corresponding to critical case Minimum eigen value 0.5507

Bus no.	IVI (pu)	δ (degree)	P_G (MW)	Q_G (Mvar)	L index
1	1.010	2.030	114.170	14.551	-
2	1.000	0.000	121.165	63.537	-
3	0.980	-5.516	50.000	8.909	-
4	0.950	-5.713	0.000	0.000	0.0389
5	0.953	-4.595	0.000	0.000	0.0272
6	0.990	-11.909	0.000	7.451	-
7	0.966	-10.396	0.000	0.000	0.0555
8	1.000	-10.396	0.000	13.332	-
9	**0.944**	-12.976	0.000	0.000	**0.1013**
10	**0.941**	-13.251	0.000	0.000	0.0969
11	0.961	-12.731	0.000	0.000	0.0532
12	0.972	-13.037	0.000	0.000	0.0300
13	0.964	-13.137	0.000	0.000	0.0414
14	**0.932**	-14.364	0.048	0.000	**0.1067**
Total P_G =285.031 MW			Total Q_G = 134.845 Mvar		
Total P_D = 276.528 MW			Total Q_D = 92.418 Mvar		
Total P_{loss} = 8.506 MW			**Total Q_{loss}** = 42.431 Mvar		
Total reactive reserve			9.9239 Mvar		

Corresponding to all uncertain inputs mentioned in section-III of this paper, the critical case has been identified by observing the minimum eigen value of load flow jacobian in each dynamic alteration. Figure 14 shows the variation of minimum eigen value of load flow jacobian. Minimum eigen value encountered is 0.5507 and corresponding load flow results are given in table III.

The convergence of all the objective functions which are mentioned in section-V are shown in figures 15,16 and 17 respectively. Variation of the weakest bus voltage is shown in figure 18. The load flow results after the optimization are given in table-V and noteworthy changes have been observed on the voltage magnitudes, L-index, losses and reactive reserve of the system.

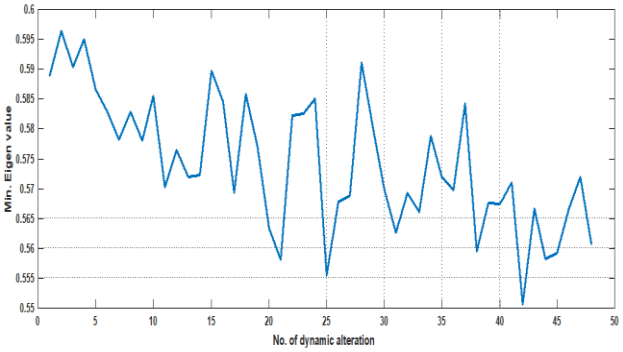

Fig.14: Variation of minimum eigen values of load flow Jacobian

Table-III shows the load flow results for the critical case and it can be observed that voltage profile at buses 9,10 and 14 are below the allowable range of voltage. Total reactive reserve in the system under stressed condition is $Q_{reserve}$ = 9.9239 Mvar which is calculated by eq. (26). Buses 9 and 14 are the weakest buses in the system since their L-index are higher as compare to remaining buses. Thus, these buses have been chosen as the candidate buses for the placement of compensating devices. The 'Black Hole Optimization Algorithm' has been applied to solve the multi-objective optimization problem and the optimization results are shown in table-IV. Total number of iterations are 100 and the population size per iteration is 100.

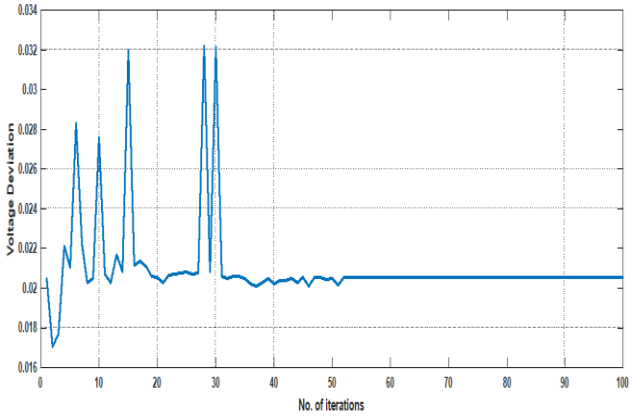

Fig. 15: Convergence of voltage deviation

Table-IV: Optimization Results

Optimized value of control variables	Q_{sh9} = 16.282 Mvar
	Q_{sh14} = 15.8740 Mvar
Objective function-1	0.0208
Objective function -2	8.114
Objective function-3	0.0944
Total reactive support in the system	32.156 Mvar
Improvement in reactive reserve	28.3493 Mvar
Total no. of iterations	100
Population size per iteration	100
CPU time	18.091654 seconds

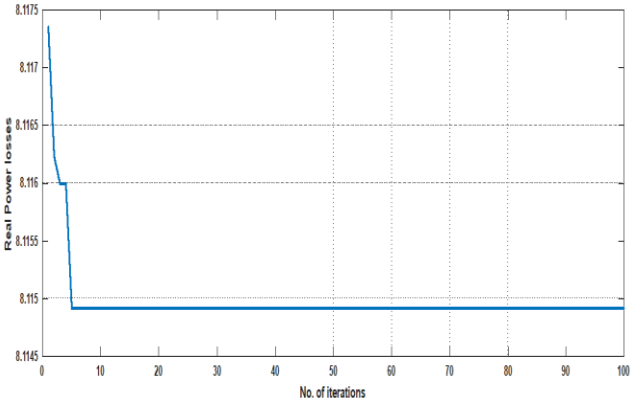

Fig. 16: Convergence of real power losses

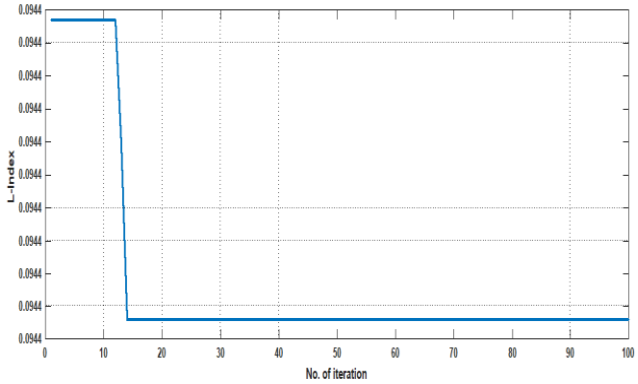

Fig. 17: Convergence of L-Index

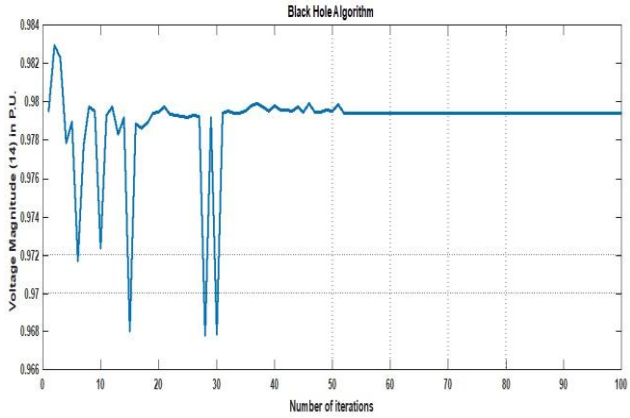

Fig. 18: Variation of voltage at bus no. 14

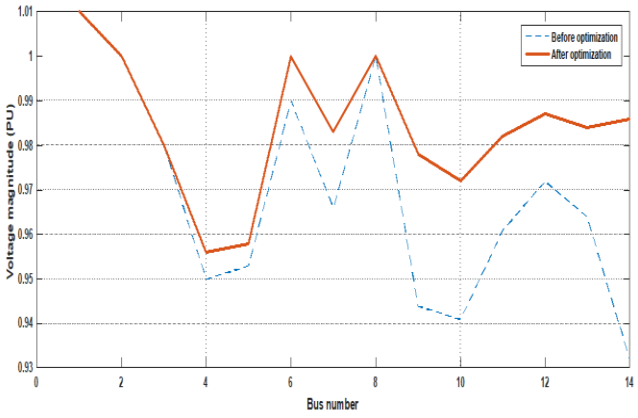

Fig. 19: Voltage profile buses before and after optimization

Table-V: Load flow results after optimization for critical case

Minimum Eigen value=0.5868

Bus no.	IVI (pu)	δ (degree)	P_G (MW)	Q_G (Mvar)	L-index
1	1.010	2.026	114.170	11.782	-
2	1.000	0.000	120.422	35.321	-
3	0.980	-5.846	50.000	35.218	-
4	0.956	-5.907	0.000	0.000	0.0380
5	0.958	-4.735	0.000	0.000	0.0266
6	1.000	-11.434	0.000	8.141	-
7	0.983	-10.317	0.000	0.000	0.0490
8	1.000	-10.317	0.000	9.585	-
9	0.978	-12.634	0.000	0.000	**0.0860**
10	0.972	-12.837	0.000	0.000	0.0821
11	0.982	-12.283	0.000	0.000	0.0457
12	0.987	-12.514	0.000	0.000	0.0267
13	0.984	-12.772	0.000	0.000	0.0367
14	0.979	-14.503	0.048	0.000	**0.0944**
Total P_G =284.640 MW			Total Q_G = 100.048 Mvar		
Total P_D = 276.528 MW			Total Q_D = 92.418 Mvar		
Total P_{loss} = 8.114 MW			**Total Q_{loss}** = 39.789 Mvar		
Total reactive reserve			38.2732 Mvar		

Table-VI: L-Index (Lines) before and after optimization

Line no.	L-index Before optimization	L-index After optimization
1	0.0318	0.0318
2	0.1381	0.1178
3	0.0176	0.0182
4	0.1351	0.1092
5	0.1419	0.1216
6	0.1203	0.0956
7	0.0171	0.0124
8	0.0148	0.0628
9	0.0647	0.0529
10	0.0337	0.0243
11	0.1119	0.0706
12	0.0714	0.0496
13	0.1013	0.0606
14	0.1479	0.0699
15	0.0792	0.0116
16	0.0096	0.0255
17	0.0438	0.0391
18	0.0874	0.0428
19	0.0319	0.0125
20	0.1240	0.0135

The comparison of bus voltages and L-Index (bus) before and after the optimization are shown in figures 19 and 20 respectively. The Voltage benefit factors (VBF) and Loss benefit factor (LBF) are given in table-VII. Theses factors are calculated by using eq. (27) and (28) respectively.

Table-VII: %VBF and %LBF

Bus no.	VBF (%)	Bus no.	VBF (%)
4	1.866	11	6.531
5	1.555	12	4.665
7	5.287	13	6.220
9	10.573	14	14.616
10	9.640	**LBF=1.024%**	

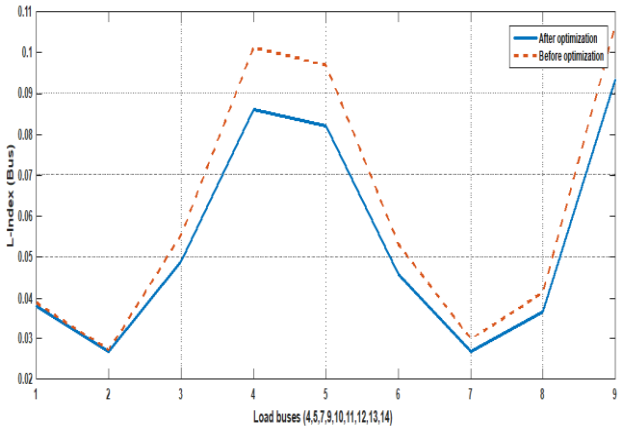

Fig. 20: L-Index (bus) before and after optimization

VII. CONCLUSION

The handling, representation and consequences of load uncertainties have been discussed in this paper. Along with uncertain loads distributed generations have also been considered as a source of load uncertainties. An optimal power flow has been achieved by designing a multi-objective optimization problem to improve system voltage stability and reduce the real power losses has been proposed in this paper. An optimal load Black Hole optimization algorithm has been used to solve the proposed problem. The propose technique has been implemented on IEEE-14 bus system.

APPENDIX

Air flow and Solar irradiance [24]

S.no.	Air flow (m/s)	Solar irradiance (W/m^2)	S.no.	Air flow	Solar irradiance
1	0.5	690.3	25	18.0	635.3
2	1.1	735.2	26	19.3	635.3
3	2.0	741.2	27	20.0	623.5
4	2.5	758.8	28	20.5	605.9
5	3.2	723.5	29	21.0	600
6	3.5	758	30	22.0	588.2
7	4.1	720.5	31	23.0	588.2
8	5.0	705.9	32	24.4	588.2
9	5.5	711.8	33	25.0	588.2
10	6.0	700	34	26.0	582.4
11	7.0	700	35	27.0	564.7
12	7.8	694.1	36	28.0	547.1
13	8.0	688.2	37	29.3	541.2
14	9.0	682.4	38	30.0	541.2
15	9.8	682.4	39	30.6	541.2
16	10.2	682.4	40	31.0	529.4
17	11.0	676.5	41	32.3	529.4
18	12.0	664.7	42	33.0	517.6
19	13.0	664.7	43	34.0	511.8
20	14.5	670.6	44	34.8	500
21	15.0	658.8	45	35.0	482.4
22	16.2	652.9	46	36.7	441.2
23	16.5	652.9	47	38.0	423.5
24	17.0	647.1	48	40.0	394.1

ACKNOWLEDGMENT

Authors are highly acknowledged to Prof. L.D. Arya (Former Professor at SGSITS Indore), Prof. L.S. Titare (Professor at JEC Jabalpur) and Dr. Pushpendra Singh (Assistant Professor at Rajkiya Engineering College, Banda) for their continuous motivation and support towards entire research work.

REFERENCES

1. Allan, Ronald N., 'Reliability evaluation of power systems', Springer Science & Business Media, 2013.
2. Helton J.C., Johnson J.D., Sallaberry C.J. and Storlie C.B., 'Survey of sampling-based methods for uncertainty and sensitivity analysis', Reliability Engineering & System Safety, 2006, 91, (10-11), pp. 1175-1209.
3. Lomei H., Sutanto D., Muttaqi K. M. and Alfi A., 'An Optimal Robust Excitation Controller Design Considering the Uncertainties in the Exciter Parameters', IEEE Transactions on Power Systems, 2017, 32, (6), pp. 4171-4179.
4. Chen B. and Wang L., 'Robust Transmission Planning Under Uncertain Generation Investment and Retirement', IEEE Transactions on Power Systems, 2016, 31, (6), pp. 5144-5152.
5. Chassin FS, Forrest S., Ebony T. Mayhorn, Marcelo A. Elizondo, and Shuai Lu. 'Load modelling and calibration techniques for power system studies', North American Power Symposium (NAPS), 2011, pp. 1-7.
6. Zhang T., Sheng W., Song X., Meng X. and Shi C., 'Probabilistic Modelling and Simulation of Stochastic Load for Power System Studies', UK Sim 15th International Conference on Computer Modelling and Simulation, Cambridge, 2013, pp.
7. 519-524.
8. Sauer PW, Pai MA. 'Power system dynamics and stability', Urbana, 1998.
9. Sharma N.K., Choube S.C., Varma A., 'Tweak of Voltage Profile Considering Uncertain Load Models in Power Systems Using TLBO', International Journal of Engineering Trends and Technology (IJETT), 2018, 55, (2), pp. 48-55.
10. Ian A. Hiskens, Jassim Alseddiqui, "Approximation and Uncertainty in Power System Dynamic Simulation", IEEE Transactions on Power Systems, vol. 21, no. 4, pp.1808-1820, 2006.
11. M. Ali, M. Pant, A. Abraham, "A Modified Differential Evolution Algorithm and its Application to Engineering Problems", 2009 International Conference of Soft Computing and Pattern Recognition, IEEE Computer Society, 987-0-7695- 3879-2/09, 2009.
12. A. Hatamlou, "Blackhole: A New Heuristic Optimization Approach for Data Clustering", Information Sciences Elsevier, 222, 175–184, 2013.
13. D.Karlsson, D.J.Hill, "Modelling and identification of nonlinear dynamic loads in power systems", IEEE Trans. Power Syst., vol. 9, (1), pp. 157–166, 1994.
14. W.Xu, Y.Mansour, "Voltage stability analysis using generic dynamic load models", IEEE Trans. Power Syst., vol. 9, (1), pp. 479–493,1994.
15. P. Zhang, S. T. Lee, "Probabilistic load flow computation using the method of combined cumulants and Gram-Charlier expansion", IEEE Trans Power Systems, vol. 19, issue. 1, pp. 676 – 682, 2004.
16. P. C. Stern, "What Psychology Knows About Energy," What psychology knows about energy conservation, vol. 47, no. 10, 1992.
17. J. Zhu, "Optimization of Power System Operation", John Wiley Publication, 2009.

18. H. Yu, C. Y. Chung, K. P. Wong and J. H. Zhang, "A Chance Constrained Transmission Network Expansion Planning Method With Consideration of Load and Wind Farm Uncertainties", IEEE Transactions On Power Systems, Vol. 24, No. 3, Aug. 2009.
19. Rajesh Karki, PoHu, and Roy Billinton, "A Simplified Wind Power Generation Model for Reliability Evaluation" IEEE Transactions on Energy Conversion, 2006, vol. 21, no. 2, 533-540.
20. Roy Billinton, Yi Gao, "Multistate Wind Energy Conversion System Models for Adequacy Assessment of Generating Systems Incorporating Wind Energy" IEEE Transactions on Energy Conversion, 2008, vol. 23, pp 163-170.
21. Sheng W., Liu K., Liu Y., Meng X., Li Y., 'Optimal Placement and Sizing of Distributed Generation via an Improved Non-dominated Sorting Genetic Algorithm II', IEEE Transactions on Power Delivery, 2015, 30, (2), pp. 569-578.
22. Snegirev D. A., Valiev R.T., Eroshenko S.A., Khalyasmaa A.I., 'Functional assessment system of solar power plant energy production', International Conference on Energy and Environment (CIEM), 2017, pp. 349-353.
23. P. Kessel, H. Glavitsch, "Estimating the Voltage Stability of a Power System", IEEE Power Engineering Review, Volume: PER-6, Issue: 7, pp. 72, 1986.
24. G B Jasmon, L H C C Lee, "Distribution Network Reduction for Voltage Stability Analysis and Load Flow Calculations", Electrical Power and Energy Systems, Volume: 13, Issue: 1, pp. 1–3, 1991.
25. School of Energy and environment technology, RGPV Bhopal.

AUTHORS PROFILE

Namami Krishna Sharma is currently pursuing Ph.D. from UIT-RGPV Bhopal. His research areas are Power system stability & control, soft computing techniques and uncertainty analysis in power systems. He published several papers in reviewed journals and reputed conferences.

Prof. S. C. Choube is the Professor in Electrical & Electronics engineering department of UIT-RGPV, Bhopal. He published various research papers in Reputed journals and reputed conferences. His research area includes Power system voltage stability, modern optimization techniques, power system reliability and security analysis. He is the active member of various professional bodies.